

Mechanistic investigation of energy transfer in perylene-cored anthracene dendrimers†

Masaki Takahashi,*^a Hironao Morimoto,^b Kentaro Miyake,^a Hideki Kawai,^c Yoshihisa Sei,^d Kentaro Yamaguchi,^d Tetsuya Sengoku^a and Hidemi Yoda*^a

Received (in Durham, UK) 1st November 2007, Accepted 6th December 2007

First published as an Advance Article on the web 2nd January 2008

DOI: 10.1039/b716908f

In this publication, we describe results of investigations focusing on detailed mechanisms of directed energy transfer in perylene-cored anthracene dendrimers. To obtain definitive statistical data for probing the energy transfer pathways, we synthesized four analogous dendrimers, which were designed to funnel the energy only from remote anthracene groups to the perylene cores. Static fluorescence studies with these dendrimers revealed that excitation of the anthracene groups led to the core emissions, indicating efficient energy transfer should be involved. Inspection of the energy transfer efficiencies obtained from all ten dendrimers demonstrated that single-step energy transfer should represent a key mechanism for the long-range energy transport in these dendrimers.

Introduction

Natural photosynthetic organisms have developed the most sophisticated light harvesting systems that contain large numbers of porphyrins held in particular three-dimensional arrays. The highly ordered structure of the antenna pigments in the nanoscopic domains plays a key role in efficient transport of the solar energy to a reaction center that ultimately achieves solar energy conversion.¹ In order to mimic the function of the natural light-harvesting antenna systems, considerable effort has been directed towards designing and synthesizing artificial structures containing donor and acceptor chromophoric units in supramolecular and dendritic systems.^{2,3} Nevertheless, photophysical characteristics of the light-harvesting dendrimer systems have remained a standing concern due to the fact that these nanoscopic-sized multichromophoric assemblies result in mechanistic complexities of the excited-state behavior arising from many excitonic interactions between neighboring chromophores.⁴ In previous publications, we have reported a series of perylene-cored anthracene dendrimers **1–6** (Fig. 1), which exhibited light-harvesting functionalities from peripheral anthracene groups to the perylene cores.^{5,6} During the course of our studies we found that energy transfer efficiencies were

unaffected by relative orientation of the donor and acceptor chromophores within the dendrimer domains. In the present publication, we describe the results of continuing investigations, which delineate the mechanism of energy transfer in the multichromophore systems. A key to successful implementation of the plan was a consideration of possible pathways available to long-range energy transfer from the remote anthracene donor groups to the perylene cores: direct (single-step) and indirect (multistep) pathways could be envisaged. To resolve this mechanistic problem, we prepared and studied four simplified dendrimer analogues **7–10** incorporating 1,4-disubstituted benzene moieties as an interlinking interior unit. As a result of detailed analyses of energy transfer efficiencies, we clearly demonstrated that the single-step energy transfer was the major pathway in the dendrimer systems.

Results and discussion

The construction of new dendritic structures (**7–10**) was successfully achieved by direct coupling of peripheral (**A1** and **A2**) and core fragments (**P1** and **P2**), using our previous strategy for preparations of anthracene-based dendrimers (Scheme 1).^{5–7} Since we have established the synthetic approaches to **P1** and **P2**, our initial focus was the synthesis of **A1** and **A2** following the previous synthetic routes with slight structural modifications.⁶ The synthesis of **A1** and **A2** started with free radical bromination of commercially available methyl 4-methylbenzoate **11** (Scheme 2). Upon treatment of **11** with NBS/AIBN, the methyl group was converted to the corresponding bromomethyl functionality, giving methyl 4-(bromomethyl)benzoate **12** as a predominant product (87%). This synthetic intermediate underwent nucleophilic substitution reactions with 3-benzoyloxyphenol and 3,5-dibenzoyloxyphenol to afford **13L** and **13B** in 91% and 92% yield, respectively. The benzoyl groups of these substances were chemoselectively removed with *n*-butylamine to give **14L** (85%) and **14B** (83%) without affecting the ester endgroups.

^a Department of Materials Science, Faculty of Engineering, Shizuoka University, 3-5-1 Johoku, Naka-ku, Hamamatsu, Shizuoka 432-8561, Japan. E-mail: tmtakah@ipc.shizuoka.ac.jp, tchyoda@ipc.shizuoka.ac.jp; Fax: +81-53-478-1621, +81-53-478-1150; Tel: +81-53-478-1621, +81-53-478-1150

^b Graduate School of Science and Engineering, Shizuoka University, 3-5-1 Johoku, Naka-ku, Hamamatsu, Shizuoka 432-8561, Japan

^c Research Institute of Electronics, Shizuoka University, 3-5-1 Johoku, Naka-ku, Hamamatsu, Shizuoka 432-8011, Japan

^d Faculty of Pharmaceutical Sciences at Kagawa Campus, Tokushima Bunri University, Shido, Sanuki, Kagawa 769-2193, Japan

† Electronic supplementary information (ESI) available: Table for SEC results (Table S1); plot for SEC results (Fig. S1); synthetic details and complete characterization data for the synthetic intermediates (**A1**, **A2** and **12–16**); ¹H and ¹³C NMR spectra (**A1**, **A2**, **7–10** and **12–16**); SEC traces (**7–10**). See DOI: 10.1039/b716908f

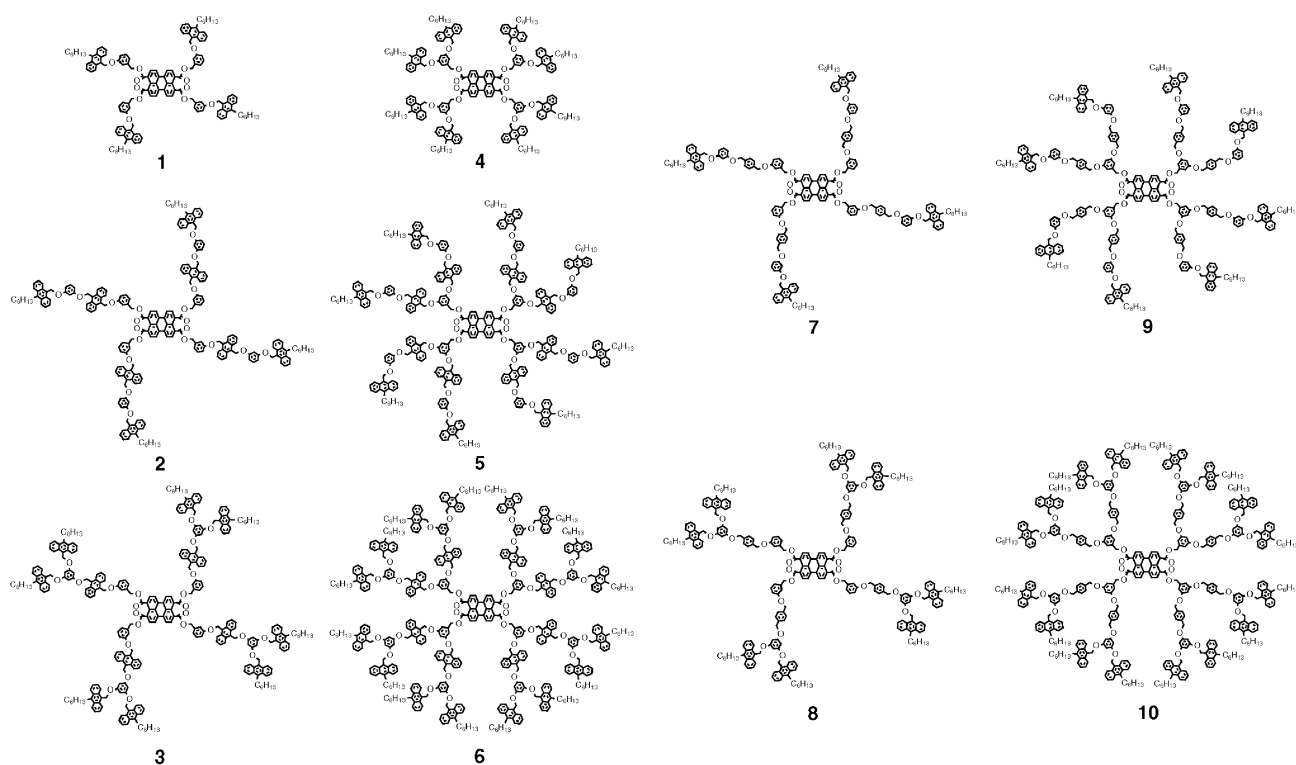


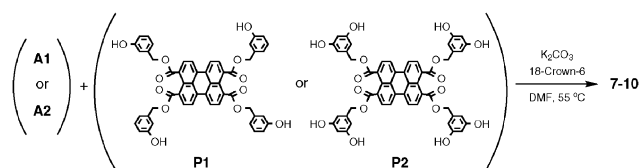
Fig. 1 Structures of 1–10.

These intermediates were then subjected to reaction with 9-(chloromethyl)-10-hexylanthracene under conditions used for the other anthracenemethyl ethers^{5–7} to yield **15L** (88%) and **15B** (87%). The methoxycarbonyl groups of these molecules were readily reduced with lithium aluminum hydride, rendering the corresponding benzylic alcohols **16L** (98%) and **16B** (91%). Finally, treatment of these compounds with methanesulfonyl chloride and an excess of lithium chloride led to efficient production of **A1** (96%) and **A2** (93%).

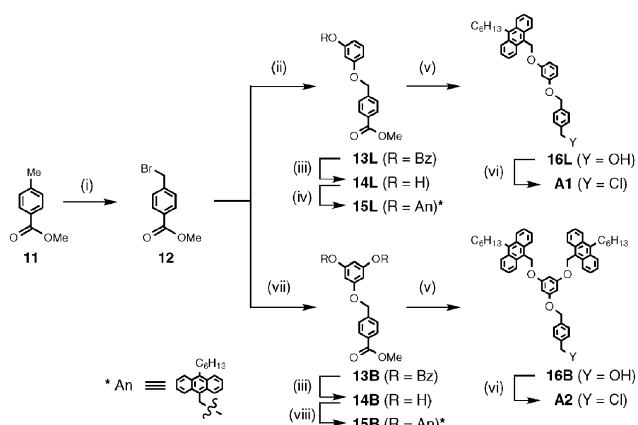
With these dendritic fragments in hand, we synthesized **7–10** by combinatorial method employing direct coupling reactions of the peripheral (**A1** and **A2**) and core (**P1** and **P2**) fragments at the multiple reaction sites. These dendrimers were satisfactorily characterized by elemental analyses and a range of spectroscopies. To obtain further structural information about polydispersity indices and molecular masses for these macromolecular systems, size exclusion chromatography (SEC) was examined (Table S1, see ESI†). From the SEC data obtained from 10 individual dendrimers and 6 individual polystyrene standards, it appears that all the dendrimers gave low polydispersity values ($M_w/M_n < 1.1$), being in the range found for monodisperse structures with a precisely controlled number of functional groups.⁸ Fig. S1 (see ESI†) shows semilogarithmic

plots of molecular weight values vs. SEC retention volumes (V) for the examined compounds, which are almost linear and have a unified downward slope. On the basis of this correlation, the molecular weight values for **1–10** were approximated through calibration with the polystyrene standards. Apparently, the estimated molecular weights (M_w) proved to be sufficiently close to the nominal values for smaller and medium-sized dendrimers (entries 1–5 and 7–9), whereas larger-sized dendrimers gave considerably underestimated M_w values (entries 6 and 10). It is well-established that dendritic structures give smaller M_w values than their actual molecular weights particularly for higher-generation dendrimers.⁸ Therefore, it is clear that the SEC experiments were consistent with the formation of **7–10**, providing a convincing evidence that our synthetic strategy could be applied in the construction of these covalently bound multichromophore systems.

The presence of the precise number of chromophores in **7–10** was confirmed by UV-Vis spectroscopy, which exhibited three absorption bands assigned to the anthracene groups in a shorter-wavelength region (350–410 nm) and two absorption bands assigned to the perylene groups in a longer-wavelength region (430–500 nm) as we have previously observed for **1–6** (Fig. 2 and Table 1). In Fig. 3, representative absorption coefficients of both chromophores were plotted as a function of the total number of anthracene groups. Throughout the series of **1–10**, the absorption coefficients for anthracene at 359 nm exhibited a linear relationship passing through the origin, while those for perylene at 477 nm were approximately constant. These results indicated that a number of the chromophores held in the dendritic arrays behaved as non-interacting monomeric species that could be distinguished in the



Scheme 1



Scheme 2 Reagents and conditions: (i) NBS, AIBN, CHCl₃, reflux; (ii) 3-(benzyloxy)phenol, 18-crown-6, K₂CO₃, DMF, 55 °C; (iii) *n*-BuNH₂, THF, reflux; (iv) 9-(chloromethyl)-10-hexylanthracene (1 equiv.), 18-crown-6, K₂CO₃, DMF, 55 °C; (v) LAH, THF, rt; (vi) LiCl, MsCl, Et₃N, THF, rt; (vii) 3,5-di(benzyloxy)phenol, 18-crown-6, K₂CO₃, DMF, 55 °C; (viii) 9-(chloromethyl)-10-hexylanthracene (2 equiv.), 18-crown-6, K₂CO₃, DMF, 55 °C.

absorption spectra. Thus, the precise stoichiometry of the chromophoric groups was unambiguously verified through these investigations, providing definitive support for all the dendrimer structures.

Fig. 4 shows steady-state fluorescence and excitation spectra of 7–10 in chloroform solutions. In the fluorescence emission spectra (Fig. 4(A)), these dendrimers displayed significant perylene emission bands in a longer-wavelength region (470–600 nm) and weak anthracene emission bands in a shorter-wavelength region (400–450 nm) upon excitation of the anthracene chromophores at 378 nm. Furthermore, the excitation spectra obtained at λ_{em} of the core at 500 nm (Fig. 4(B)) were found to be similar in shape to their absorption spectra, which exhibited three sharp peaks characteristic of the anthracene groups in the shorter-wavelength region (350–410 nm) and two clearly structured peaks characteristic of the perylene groups in the longer-wavelength region (430–500 nm). These observations were consistent with a mechanism which involved intramolecular energy transfer driven by donor–acceptor interactions between the peripheral anthracene groups and the perylene cores.^{5,6} It should be noted that fluorescence emissions arising from the anthracene periphery showed different degrees of relative intensity (Table 1), which may distinguish two dendrimers 9 and 10 from the others. In these systems, the dendritic backbones may serve as sterically demanding spacers that keep the anthracene groups away from the perylene core, restricting possibilities of energy redistribution around the excited donors. On the contrary, it can be deduced that suppression of the donor emissions observed for 1–8 was indicative of increased exciton delocalization processes, since the excited donor groups could be in close contact with neighboring chromophores and have a tendency to interact each other.

To understand the mechanistic scheme taking place in the dendrimers, examination of energy transfer efficiencies (ϕ_{ET}) would indicate fundamental aspects of the energy transfer processes.⁹ By comparing the donor peaks in the excitation spectra of the dendrimers with those in the absorption spectra

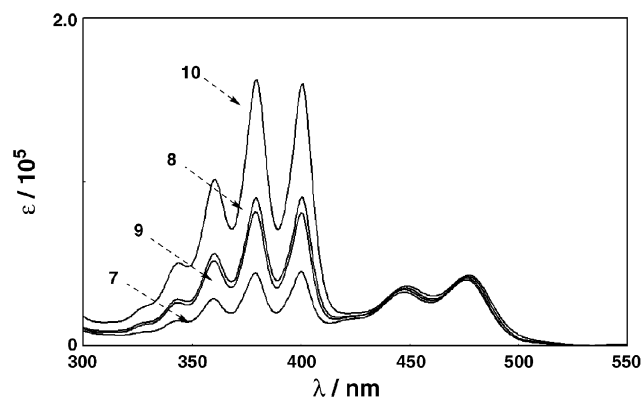


Fig. 2 Absorption spectra of 7–10 in chloroform solutions.

normalized for the acceptor peaks, the ϕ_{ET} values for 7, 8, 9 and 10 were estimated to be 0.63, 0.65, 0.58 and 0.55, respectively,¹⁰ which were summarized together with those previously reported for 1–6 in Table 1.⁶ In Fig. 5, we plotted all these ϕ_{ET} data as a function of the number of anthracene chromophores incorporated at the periphery of the dendrimers. As can be seen from the figure, the ϕ_{ET} values were found to be fitted into two distribution patterns, where lower-density dendrimers 1, 2, 3, 7 and 8 gave superior quantum efficiencies to higher-density dendrimers 4, 5, 6, 9 and 10. In this context, it has been recognized that dendritic architectures functionalized with anthracene clusters gave rise to decreased photoluminescence quantum efficiencies.⁷ This observation may be connected with aggregated nature of the multichromophore systems which promote radiationless deactivation through excited state interactions between chromophores. Based on this consideration, the observed difference in ϕ_{ET} values between the lower- and higher-density dendrimers could be reasonably explained by the mechanism of energy migration between branches of the dendrimers. Of particular interest in the course of our investigations were molecular structure–property relationships that would govern the energy transfer efficiencies and provide mechanistic information about the energy transfer processes. Remarkably, the ϕ_{ET} values for the dendrimers 2, 3, 5 and 6 were nearly equal to those for the benzyl-ether counterparts 7, 8, 9 and 10, respectively, indicating that the interior anthracene donor groups present near the cores did not play a role in long-range energy transfer from the exterior donors to the acceptors. An interpretation of this result was that at any donor–acceptor distance the energy transfer occurred in a single-step manner within the dendritic shells, because the multistep mechanism was no longer efficient. Another remarkable finding was that the ϕ_{ET} values for 7 and 9 were almost the same as those for 1 and 4, respectively. In fact, averaged distances for the short- and long-range energy transfer were estimated to be 1.4 and 2.3 nm, respectively, by means of molecular modeling studies performed on fully extended structures of 1–10.⁶ The obvious conclusion which could be drawn from these considerations was that the energy transfer efficiencies at the two different donor–acceptor distances were essentially equal. This conclusion is intriguing when one considers the Förster relation that scales energy transfer efficiency with the inverse sixth power of

Table 1 UV-Vis and fluorescence data and energy transfer efficiencies for 1–10

Entry	λ_{\max}/nm ($\epsilon/10^4$) ^a	$\lambda_{\text{em}}/\text{nm}$ (I) ^b	ϕ_{ET} ^c
1	342 (1.21), 359 (2.29), 378 (3.56), 399 (3.74), 446 (3.49), 475 (4.26)	409 (0.03), 431 (0.03), 493 (1.00), 524 (0.64)	0.69 ^d
2	340 (2.48), 357 (4.81), 375 (7.30), 396 (7.34), 448 (3.44), 477 (4.14)	409 (0.02), 432 (0.02), 493 (1.00), 525 (0.63)	0.69 ^d
3	342 (3.63), 358 (7.32), 377 (11.4), 398 (11.4), 448 (3.40), 476 (4.14)	410 (0.02), 432 (0.02), 494 (1.00), 524 (0.61)	0.65 ^d
4	343 (2.32), 360 (4.62), 378 (7.30), 399 (7.32), 448 (3.47), 477 (4.22)	409 (0.04), 432 (0.06), 493 (1.00), 525 (0.69)	0.54 ^d
5	342 (5.00), 358 (9.64), 376 (14.8), 397 (14.6), 449 (3.57), 477 (4.19)	409 (0.02), 433 (0.03), 495 (1.00), 527 (0.69)	0.54 ^d
6	342 (7.00), 359 (14.1), 378 (22.4), 399 (22.3), 449 (3.63), 478 (4.33)	411 (0.02), 432 (0.02), 495 (1.00), 526 (0.64)	0.48 ^d
7	342 (1.52), 359 (2.84), 378 (4.43), 399 (4.54), 447 (3.25), 477 (4.03)	408 (0.09), 431 (0.09), 493 (1.00), 525 (0.63)	0.63
8	342 (2.75), 359 (5.50), 378 (8.80), 399 (8.87), 447 (3.42), 477 (4.14)	408 (0.04), 431 (0.04), 493 (1.00), 525 (0.57)	0.65
9	342 (2.54), 359 (5.12), 378 (8.11), 399 (8.06), 447 (3.50), 477 (4.23)	409 (0.50), 431 (0.48), 493 (1.00), 525 (0.58)	0.58
10	342 (4.82), 359 (9.84), 378 (15.8), 399 (15.5), 447 (3.59), 477 (4.31)	409 (0.63), 431 (0.62), 493 (1.00), 525 (0.56)	0.55

^a Absorption wavelengths (λ_{\max}) and absorption coefficients (ϵ) for the absorption maxima. The ϵ values were determined by measurements employing chloroform solutions of the samples, where all calibrations were linear in the range from 1 to 20 $\mu\text{mol L}^{-1}$. ^b Emission wavelengths (λ_{em}) and signal intensities (I) for the fluorescence emission maxima. The I values represent fluorescence intensities relative to those for the highest fluorescence peaks around 494 nm. ^c Quantum efficiencies for energy transfer. The ϕ_{ET} values were determined by comparison between the absorption spectra and the excitation spectra, see ref. 10. ^d See ref. 6.

the donor–acceptor distances.¹¹ The observed distance independence in energy transfer efficiency could be rationalized by taking into account the Förster critical radius (R_0) of 3.6 nm that has been previously reported for the anthracene–perylene pair.¹² Using this parameter in the Förster relation, we could make simple estimations of the ϕ_{ET} values for the short- and long-range energy transfer processes, which were found to be almost equivalent.¹³ The results discussed above indicated that the dendrimer domains confined within the Förster critical radius served as a unique molecular environment that ensured the efficient pathways for the single-step energy transfer.

Conclusions

We have investigated the mechanistic aspects of the energy transfer in the perylene-cored anthracene dendrimers through inspection of the energy transfer efficiencies. The results of these studies led to the definitive conclusion that all the competitive energy transfer processes occurred in the single-step manner. Another remarkable finding was that variations in the interchromophore distance between the donor and acceptor groups had no influence on the efficiencies of energy transfer processes occurring within the nanoscopic dimension of dendritic architectures. Consequently, the mechanistic studies described here exemplify the fundamental importance of

nanoscopic energy transfer properties for the fabrication of superior light-harvesting materials, which can facilitate future device applications in the areas of photonics,¹⁴ sensors,¹⁵ and solar energy conversion.¹⁶

Experimental

General:

All solvents and reagents were of reagent grade quality from Wako Pure Chemicals used without further purification. The

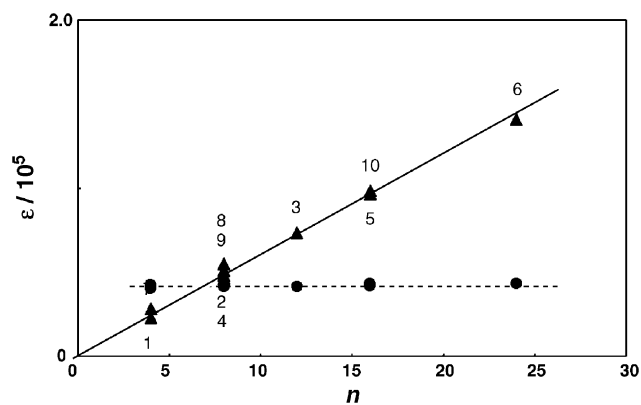


Fig. 3 Plots of extinction coefficients (ϵ) at 359 nm (\blacktriangle , solid line) and at 477 nm (\bullet , dotted line) vs. the total number of anthracene units (n) for 1–10.

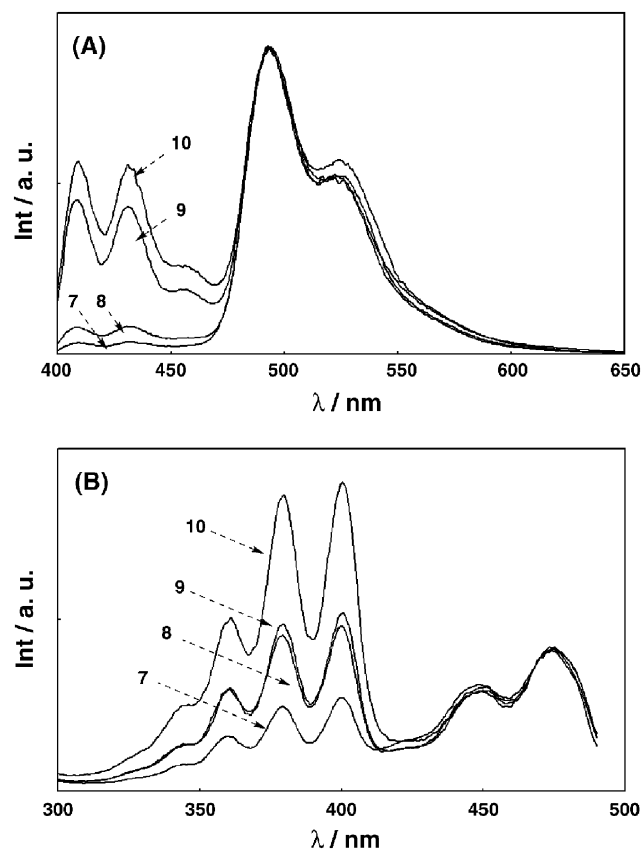


Fig. 4 (A) Fluorescence spectra ($\lambda_{\text{ex}} = 378$ nm, normalized at 500 nm) and (B) excitation spectra of 7–10 ($\lambda_{\text{em}} = 500$ nm, normalized at 470 nm) in chloroform solutions.

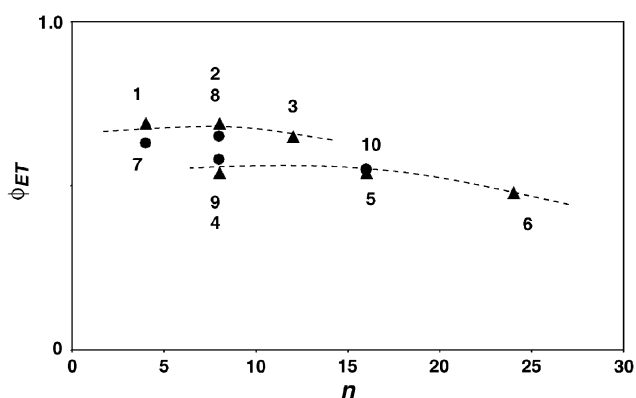


Fig. 5 Plots of energy transfer efficiencies (ϕ_{ET}) vs. the total number of anthracene units (n) in the dendrimer systems 1–6 (▲) and 7–10 (●).

^1H - and ^{13}C -nuclear magnetic resonance (NMR) spectra operating at the frequencies of 300 and 75 MHz, respectively, were recorded on a JEOL JNM-AL300 spectrometer in chloroform- d (CDCl_3) or acetone- d_6 ($(\text{CD}_3)_2\text{CO}$). Chemical shifts are reported in parts per million (ppm) relative to TMS and the solvent used as internal standards, and the coupling constants are reported in hertz (Hz). Fourier transform infrared (FT-IR) spectra were recorded on a JASCO FT/IR-410 spectrometer as KBr disks. UV-Vis and fluorescence spectra were recorded on a JASCO model V-570 UV-VIS-NIR spectrophotometer and a Hitachi F-4500 spectrofluorometer, respectively. These measurements were carried out in sufficiently low concentrations (10^{-8} – 10^{-5} M) of the analytes to exclude the possibilities of intermolecular chromophoric interactions. Melting points were measured with a Yanaco MP-S3 melting point apparatus. Fast atom bombardment (FAB) mass spectra were obtained on a JASCO JMS-HX110A using a 3-nitrobenzyl alcohol matrix. Electrospray ionization-time-of-flight (ESI-TOF) mass spectra were obtained on a Micromass LCT mass spectrometer KB 201. Cold-spray ionization mass spectrometry (CSI-MS) was performed by two-sector (BE) mass spectrometer (JMS-700, JEOL) equipped with a cold-spray ionization (CSI) source. Elemental analyses were performed by Thermo Flash EA 1112 instrument. Size exclusion chromatography (SEC) was performed by a system consisting of a JASCO model 880-PU pump at a flow rate of $0.5\text{ cm}^3\text{ min}^{-1}$ and JASCO 875-UV absorbance detector (254 nm) equipped with a Shodex K-802.5 column (chloroform as eluent). Preparative HPLC purification was performed by a Japan Analytical Industry LC-918 recycling system. Since singly charged molecular ion peaks of **9** and **10** could not be detected by all available mass spectral techniques (FAB, MALDI-TOF, ESI and CSI), the SEC analyses were applied to the molecular weight determinations for these compounds.

Dendrimer 7

A solution containing **A1** (0.11 g, 0.21 mmol), **P1** (0.029 g, 0.034 mmol), potassium carbonate (0.028 g, 0.20 mmol) and 18-crown-6 (0.054 g, 0.20 mmol) in DMF (7 cm^3) was heated at $55\text{ }^\circ\text{C}$ with stirring under argon atmosphere. After 4 h, the

reaction mixture was cooled to room temperature, and poured into saturated ammonium chloride solution (100 cm^3) to precipitate the product. The precipitate was collected by filtration, intensively washed with water, and dried in a vacuum. Purification of the residue by the preparative HPLC (chloroform as eluent) gave **7** (0.056 g, 59%) as an orange-colored powder (Found: C, 82.2; H, 6.1. $\text{C}_{192}\text{H}_{172}\text{O}_{20}$ requires C, 82.4; H, 6.2%); mp 92 – $93\text{ }^\circ\text{C}$ (from chloroform–hexane); $\nu_{\text{max}}(\text{KBr})/\text{cm}^{-1}$ 1589 (C=C) and 1716 (CO); m/z (ESI) 2823 (1%, $\text{M} + \text{Na}^+$), 640 (43), 588 (33), 275 (88) and 191 (100); δ_{H} (300 MHz; CDCl_3 ; Me_4Si) 0.91 (12H, t, J 7.0, $(\text{CH}_2)_5\text{CH}_3$), 1.28–1.42 (16H, m, $(\text{CH}_2)_3(\text{CH}_2)_2\text{CH}_3$), 1.50–1.62 (8H, m, $(\text{CH}_2)_2\text{C}-\text{H}_2(\text{CH}_2)_2\text{CH}_3$), 1.69–1.85 (8H, m, $\text{CH}_2\text{CH}_2(\text{CH}_2)_3\text{CH}_3$), 3.55 (8H, t, J 8.1, $\text{CH}_2(\text{CH}_2)_4\text{CH}_3$), 4.94 (8H, s, OCH_2), 4.97 (8H, s, OCH_2), 5.25 (8H, s, OCH_2), 5.81 (8H, s, OCH_2), 6.57–6.63 (4H, m, ArH), 6.70–6.77 (8H, m, ArH), 6.84–6.90 (4H, m, ArH), 6.97–7.04 (4H, m, ArH), 7.05–7.09 (4H, m, ArH), 7.18–7.27 (8H, m, ArH), 7.34 (16H, s, ArH), 7.46–7.49 (16H, m, ArH), 7.83 (4H, d, J 8.1, ArH), 7.90 (4H, d, J 8.1, ArH) and 8.18–8.30 (16H, m, ArH); δ_{C} (75 MHz; CDCl_3) 14.0 (q), 22.6 (t), 28.3 (t), 30.0 (t), 31.3 (t), 31.7 (t), 62.8 (t), 66.8 (t), 69.56 (t), 69.59 (t), 102.1 (d), 107.2 (d), 107.6 (d), 114.7 (d), 114.8 (d), 120.9 (d), 121.4 (d), 124.7 (d), 125.1 (d), 125.2 (d), 126.0 (d), 127.7 (d), 128.6 (s), 128.9 (s), 129.3 (s), 129.7 (d), 130.1 (d), 130.7 (s), 130.9 (s), 132.9 (s), 136.6 (s), 136.7 (s), 137.2 (s), 138.1 (s), 159.0 (s), 160.1 (s), 160.6 (s) and 168.2 (s).

Dendrimer 8

A solution containing **A2** (0.12 g, 0.15 mmol), **P1** (0.022 g, 0.026 mmol), potassium carbonate (0.021 g, 0.15 mmol) and 18-crown-6 (0.040 g, 0.15 mmol) in DMF (7 cm^3) was heated at $55\text{ }^\circ\text{C}$ with stirring under argon atmosphere. After 4 h, the reaction mixture was cooled to room temperature, and poured into saturated ammonium chloride solution (100 cm^3) to precipitate the product. The precipitate was collected by filtration, intensively washed with water, and dried in a vacuum. Purification of the residue by the preparative HPLC (chloroform as eluent) gave **8** (0.050 g, 49%) as an orange-colored powder (Found: C, 83.5; H, 6.5. $\text{C}_{276}\text{H}_{260}\text{O}_{24}$ requires C, 83.7; H, 6.6%); mp 123 – $124\text{ }^\circ\text{C}$ (from chloroform–hexane); $\nu_{\text{max}}(\text{KBr})/\text{cm}^{-1}$ 1591 (C=C) and 1718 (CO); m/z (ESI) 3997 (100%, $\text{M} + \text{Cl}^-$); δ_{H} (300 MHz; CDCl_3 ; Me_4Si) 0.89 (24H, t, J 7.0, $(\text{CH}_2)_5\text{CH}_3$), 1.25–1.41 (32H, m, $(\text{CH}_2)_3(\text{CH}_2)_2\text{CH}_3$), 1.47–1.61 (16H, m, $(\text{CH}_2)_2\text{CH}_2(\text{CH}_2)_2\text{CH}_3$), 1.66–1.81 (16H, m, $\text{CH}_2\text{CH}_2(\text{CH}_2)_3\text{CH}_3$), 3.51 (16H, t, J 7.0, $\text{CH}_2(\text{CH}_2)_4\text{CH}_3$), 4.89 (8H, s, OCH_2), 4.92 (8H, s, OCH_2), 5.20 (8H, s, OCH_2), 5.76 (16H, s, OCH_2), 6.42–6.46 (8H, m, ArH), 6.55–6.59 (4H, m, ArH), 6.80–6.87 (4H, m, ArH), 6.92–6.99 (4H, m, ArH), 7.00–7.06 (4H, m, ArH), 7.14–7.22 (4H, m, ArH), 7.31 (16H, s, ArH), 7.38–7.47 (32H, m, ArH), 7.71–7.84 (8H, m, ArH) and 8.15–8.27 (32H, m, ArH); δ_{C} (75 MHz; CDCl_3) 14.0 (q), 22.6 (t), 28.3 (t), 29.9 (t), 31.3 (t), 31.7 (t), 62.8 (t), 66.8 (t), 69.6 (t), 69.7 (t), 94.6 (d), 95.0 (d), 114.7 (d), 114.8 (d), 120.8 (d), 121.3 (d), 124.7 (d), 125.05 (d), 125.13 (d), 126.1 (d), 127.7 (d), 127.8 (d), 128.5 (s), 128.9 (s), 129.3 (d), 129.7 (s), 129.8 (s), 130.6 (s), 130.9 (d), 132.8 (s), 136.6 (s), 136.7 (s), 137.3 (s), 138.1 (s), 139.3 (s), 141.0 (s), 159.0 (s), 160.9 (s), 161.4 (s) and 168.2 (s).

Dendrimer 9

A solution containing **A1** (0.24 g, 0.46 mmol), **P2** (0.043 g, 0.047 mmol), potassium carbonate (0.064 g, 0.46 mmol), and 18-crown-6 (0.12 g, 0.45 mmol) in DMF (7 cm³) was heated at 55 °C with stirring under argon atmosphere. After 4 h, the reaction mixture was cooled to room temperature, and poured into saturated ammonium chloride solution (100 cm³) to precipitate the product. The precipitate was collected by filtration, intensively washed with water, and dried in a vacuum. Purification of the residue by the preparative HPLC (chloroform as eluent) gave **9** (0.099 g, 44%) as an orange-colored powder (Found: C, 82.8; H, 6.3. C₃₃₂H₃₀₈O₃₂ requires C, 82.9; H, 6.5%); mp 103–104 °C (from chloroform–hexane); $\nu_{\max}(\text{KBr})/\text{cm}^{-1}$ 1591 (C=C) and 1716 (CO); δ_{H} (300 MHz; CDCl₃; Me₄Si) 0.90 (24H, t, *J* 6.8, (CH₂)₅CH₃), 1.27–1.42 (32H, m, (CH₂)₃(CH₂)₂CH₃), 1.50–1.61 (16H, m, (CH₂)₂CH₂(CH₂)₂CH₃), 1.67–1.83 (16H, m, CH₂CH₂(CH₂)₃CH₃), 3.53 (16H, t, *J* 7.0, CH₂(CH₂)₄CH₃), 4.90 (16H, s, OCH₂), 4.91 (16H, s, OCH₂), 5.19 (8H, s, OCH₂), 5.78 (16H, s, OCH₂), 6.46–6.51 (4H, m, ArH), 6.54–6.61 (8H, m, ArH), 6.62–6.67 (8H, m, ArH), 6.67–6.75 (16H, m, ArH), 7.20 (8H, t, *J* 8.4, ArH), 7.30 (32H, s, ArH), 7.38–7.48 (32H, m, ArH), 7.87 (4H, d, *J* 8.0, ArH), 8.03 (4H, d, *J* 8.0, ArH) and 8.14–8.31 (32H, m, ArH); δ_{C} (75 MHz; CDCl₃) 14.0 (q), 22.6 (t), 28.3 (t), 30.0 (t), 31.3 (t), 31.7 (t), 62.8 (t), 66.9 (t), 69.6 (t), 69.7 (t), 102.1 (d), 107.2 (d), 107.6 (d), 121.5 (d), 122.0 (d), 124.7 (d), 125.1 (d), 125.2 (d), 126.0 (d), 127.3 (s), 127.4 (s), 127.8 (d), 129.3 (s), 130.1 (d), 130.9 (s), 136.5 (s), 136.7 (s), 138.1 (s), 139.3 (s), 141.0 (s), 160.1 (s), 160.6 (s) and 168.2 (s).

Dendrimer 10

A solution containing **A2** (0.20 g, 0.25 mmol), **P2** (0.023 g, 0.025 mmol), potassium carbonate (0.064 g, 0.46 mmol), and 18-crown-6 (0.12 g, 0.45 mmol) in DMF (7 cm³) was heated at 55 °C with stirring under argon atmosphere. After 4 h, the reaction mixture was cooled to room temperature, and poured into saturated ammonium chloride solution (100 cm³) to precipitate the product. The precipitate was collected by filtration, intensively washed with water, and dried in a vacuum. Purification of the residue by the preparative HPLC (chloroform as eluent) gave **10** (0.082 g, 46%) as an orange-colored powder (Found: C, 84.1; H, 6.8. C₅₀₀H₄₈₄O₄₀ requires C, 84.2; H, 6.8%); mp 133–134 °C (from chloroform–hexane); $\nu_{\max}(\text{KBr})/\text{cm}^{-1}$ 1593 (C=C) and 1716 (CO); δ_{H} (300 MHz; CDCl₃; Me₄Si) 0.89 (48H, t, *J* 6.8, (CH₂)₅CH₃), 1.25–1.40 (64H, m, (CH₂)₃(CH₂)₂CH₃), 1.45–1.61 (32H, m, (CH₂)₂CH₂(CH₂)₂CH₃), 1.64–1.81 (32H, m, CH₂CH₂(CH₂)₃CH₃), 3.38–3.58 (32H, m, CH₂(CH₂)₄CH₃), 4.81 (16H, s, OCH₂), 4.85 (16H, s, OCH₂), 5.13 (8H, s, OCH₂), 5.71 (32H, s, OCH₂), 6.36–6.47 (24H, m, ArH), 6.50–6.64 (12H, m, ArH), 7.18–7.31 (32H, m, ArH), 7.32–7.48 (64H, m, ArH), 7.74–8.00 (8H, m, ArH) and 8.05–8.30 (64H, m, ArH); δ_{C} (75 MHz; CDCl₃) 14.0 (q), 22.6 (t), 28.3 (t), 29.9 (t), 31.3 (t), 31.7 (t), 62.8 (t), 69.6 (t), 69.7 (t), 94.4 (d), 94.9 (d), 107.1 (d), 121.5 (d), 124.7 (d), 125.0 (d), 126.0 (d), 127.3 (d), 127.7 (d), 127.8 (d), 129.3 (s), 130.9 (s), 136.5 (s), 138.0 (s), 160.0 (s), 160.9 (s), 161.3 (s) and 168.2 (s).

Acknowledgements

This research was supported by a Grant-in-Aid for Scientific Research from the Ministry of Education, Culture, Sports, Science, and Technology, Japan and Suzuki Foundation. We thank Prof. Shuichi Hiraoka of the University of Tokyo, Japan.

References

- (a) V. Sundström, T. Pullerits and R. van Grondelle, *J. Phys. Chem. B*, 1999, **103**, 2327; (b) S. Vasil'ev, P. Orth, A. Zouni, T. G. Owens and D. Bruce, *Proc. Natl. Acad. Sci. USA*, 2001, **98**, 8602; (c) M. Z. Papiz, S. M. Prince, T. Howard, R. J. Cogdell and N. W. Isaacs, *J. Mol. Biol.*, 2003, **326**, 1523; (d) A. Amunts, O. Drory and N. Nelson, *Nature*, 2007, **447**, 58.
- (a) T. S. Balaban, *Acc. Chem. Res.*, 2005, **38**, 612; (b) A. Del Guerso, A. G. L. Olive, J. Reichwagen, H. Hopf and J.-P. Desvergne, *J. Am. Chem. Soc.*, 2005, **127**, 17984–17985; (c) K. E. Sapsford, L. Berti and I. L. Medintz, *Angew. Chem., Int. Ed.*, 2006, **45**, 4562; (d) J. A. A. W. Elemans, R. van Hameren, R. J. M. Nolte and A. E. Rowan, *Adv. Mater.*, 2006, **18**, 1251; (e) R. F. Kelley, R. H. Goldsmith and M. R. Wasielewski, *J. Am. Chem. Soc.*, 2007, **129**, 6384.
- (a) D.-L. Jiang and T. Aida, *Nature*, 1997, **388**, 454; (b) S. Gilat, A. Adronov and J. M. J. Fréchet, *Angew. Chem., Int. Ed.*, 1999, **38**, 1422; (c) A. Adronov and J. M. J. Fréchet, *Chem. Commun.*, 2000, 1701; (d) U. Hahn, M. Gorka, F. Vögtle, V. Vicinelli, P. Ceroni, M. Maestri and V. Balzani, *Angew. Chem., Int. Ed.*, 2002, **41**, 3595; (e) M. D. Yilmaz, O. A. Bozdemir and E. U. Akkaya, *Org. Lett.*, 2006, **8**, 2871.
- (a) C. Devadoss, P. Bharathi and J. S. Moore, *J. Am. Chem. Soc.*, 1996, **118**, 9635; (b) M.-S. Choi, T. Aida, T. Yamazaki and I. Yamazaki, *Angew. Chem., Int. Ed.*, 2001, **40**, 3194; (c) J. S. Melinger, Y. Pan, V. D. Kleiman, Z. Peng, B. L. Davis, D. McMorrow and M. Lu, *J. Am. Chem. Soc.*, 2002, **124**, 12002; (d) R. Métivier, F. Kulzer, T. Weil, K. Müllen and T. Basché, *J. Am. Chem. Soc.*, 2004, **126**, 14364; (e) A. Nantalaksakul, R. R. Dasari, T.-S. Ahn, R. Al-Kaysi, C. J. Bardeen and S. Thayumanavan, *Org. Lett.*, 2006, **8**, 2981; (f) T. S. Ahn, A. L. Thompson, P. Bharathi, A. Müller and C. J. Bardeen, *J. Phys. Chem. B*, 2006, **110**, 19810; (g) N. Vijayalakshmi and U. Maitra, *Macromolecules*, 2006, **39**, 7931.
- M. Takahashi, H. Morimoto, Y. Suzuki, M. Yamashita and H. Kawai, *Polym. Prepr.*, 2004, **45**, 959.
- M. Takahashi, H. Morimoto, K. Miyake, M. Yamashita, H. Kawai, Y. Sei and K. Yamaguchi, *Chem. Commun.*, 2006, 3084.
- (a) M. Takahashi, H. Morimoto, Y. Suzuki, M. Yamashita, H. Kawai, Y. Sei and K. Yamaguchi, *Tetrahedron*, 2006, **62**, 3065; (b) M. Takahashi, H. Morimoto, Y. Suzuki, T. Odagi, M. Yamashita and H. Kawai, *Tetrahedron*, 2004, **60**, 11771; (c) M. Takahashi, T. Odagi, H. Tomita, T. Oshikawa and M. Yamashita, *Tetrahedron Lett.*, 2003, **44**, 2455; (d) M. Takahashi, H. Tomita, K. Aoshima, T. Oshikawa and M. Yamashita, *Polym. Prepr.*, 2001, **42**, 282.
- (a) C. J. Hawker and J. M. J. Fréchet, *J. Am. Chem. Soc.*, 1990, **112**, 7638; (b) G. R. Newkome, C. N. Moorefield and F. Vögtle, in *Dendritic Molecules Concepts, Synthesis, Perspectives*, VCH, Weinheim, New York, Basel, Cambridge, Tokyo, 1996, pp. 1–13.
- For energy transfer dynamics, time-resolved fluorescence measurements have been performed on the dendrimers. However, attempts to record fluorescence decays failed due to limited time resolution of experimental setup (100 ps of response time).
- B. Valeur, in *Molecular Fluorescence Principles and Applications*, Wiley-VCH, Weinheim, New York, Chichester, Brisbane, Singapore, Toronto, 2002, pp. 247–272.
- N. J. Turro, in *Modern Molecular Photochemistry*, University Science Books, Sausalito, CA, 1991, pp. 298–361.
- W. H. Melhuish, *J. Phys. Chem.*, 1963, **67**, 1681.
- The energy transfer efficiency was calculated from the relation, $\phi_{\text{ET}} = 1/[1 + (r/R_0)^6]$, where r is the interchromophore distance in the structure and R_0 is the Förster critical radius for the donor-acceptor pair. Application of the above equation yielded the ϕ_{ET} values for the short- and long-range processes in a ratio of 1 : 0.94.

- 14 (a) P. K. Sudeep, B. I. Ipe, K. G. Thomas, M. V. George, S. Barazzouk, S. Hotchandani and P. V. Kamat, *Nano Lett.*, 2002, **2**, 29; (b) K. Sugiyasu, N. Fujita and S. Shinkai, *Angew. Chem., Int. Ed.*, 2004, **43**, 1229; (c) A. R. Clapp, I. L. Medintz, H. T. Uyeda, B. R. Fisher, E. R. Goldman, M. G. Bawendi and H. Mattoussi, *J. Am. Chem. Soc.*, 2005, **127**, 18212; (d) A. Huijser, T. J. Savenije, A. Kotlewski, S. J. Picken and L. D. A. Siebbeles, *Adv. Mater.*, 2006, **18**, 2234.
- 15 (a) R. Pohl, D. Aldakov, P. Kubát, K. Jursíková, M. Marquez and P. Anzenbacher, Jr., *Chem. Commun.*, 2004, 1282; (b) X. He, H. Liu, Y. Li, S. Wang, Y. Li, N. Wang, J. Xiao, X. Xu and D. Zhu, *Adv. Mater.*, 2005, **17**, 2811; (c) K. E. Sapsford, L. Berti and I. L. Medintz, *Angew. Chem., Int. Ed.*, 2006, **45**, 4562.
- 16 (a) J. M. Serin, D. W. Brousmiche and J. M. J. Fréchet, *J. Am. Chem. Soc.*, 2002, **124**, 11848; (b) S. Campagna, S. Serroni, F. Puntoriero, F. Loiseau, L. De Cola, C. J. Kleverlaan, J. Becher, A. P. Sørensen, P. Hascoat and N. Thorup, *Chem.-Eur. J.*, 2002, **8**, 4461; (c) Y. Shibano, T. Umeyama, Y. Matano, N. V. Tkachenko, H. Lemmetyinen and H. Imahori, *Org. Lett.*, 2006, **8**, 4425; (d) C. S. Karthikeyan, H. Wietasch and M. Thelakkat, *Adv. Mater.*, 2007, **19**, 1091.